Crossover behavior in failure avalanches

Srutarshi Pradhan,* Alex Hansen,† and Per C. Hemmer‡
Department of Physics, Norwegian University of Science and Technology, N-7491 Trondheim, Norway
(Received 1 December 2005; published 27 July 2006)

Composite materials, with statistically distributed thresholds for breakdown of individual elements, are considered. During the failure process of such materials under external stress (load or voltage), avalanches consisting of simultaneous rupture of several elements occur, with a distribution $D(\Delta)$ of the magnitude Δ of such avalanches. The distribution is typically a power law $D(\Delta) \propto \Delta^{-\xi}$. For the systems we study here, a crossover behavior is seen between two power laws, with a small exponent ξ in the vicinity of complete breakdown and a larger exponent ξ for failures away from the breakdown point. We demonstrate this analytically for bundles of many fibers where the load is uniformly distributed among the surviving fibers. In this case $\xi=3/2$ near the breakdown point and $\xi=5/2$ away from it. The latter is known to be the generic behavior. This crossover is a signal of imminent catastrophic failure of the material. Near the breakdown point, avalanche statistics show nontrivial finite size scaling. We observe similar crossover behavior in a network of electric fuses, and find $\xi=2$ near the catastrophic failure and $\xi=3$ away from it. For this fuse model power dissipation avalanches show a similar crossover near breakdown.

DOI: 10.1103/PhysRevE.74.016122 PACS number(s): 62.20.Mk

I. INTRODUCTION

Burst avalanches play an important role in characterizing fracture-failure phenomena [1–4]. When a weak element in a loaded material fails, the increased stress on the remaining elements may cause further failures, and thereby give a failure avalanche in which several elements fail simultaneously. With further increase in the load new avalanches occur. The statistics of such avalanches during the entire failure process explore the nature of correlations developed within the system. From the experimental point of view, failure avalanches are the only measurable quantity during the fracture-failure process of composite materials [5–7]. Under quasistatic loading, the system, with some internal load redistribution mechanism, gradually approaches the global failure point. Such damage and fracture of materials are of immense interest due to their economic and human costs. Therefore, a fundamental challenge is to find methods for providing signals that warn of imminent global failure [8]. This is of uttermost importance in, e.g., the diamond mining industry where sudden failure of a mine is always catastrophic. These mines are under continuous acoustic surveillance, but at present there is no meaningful acoustic signature of imminent disaster. The same type of question is of course central to earthquake prediction [2–4].

In this paper we will study crossover behavior of failure avalanches in the context of two very different models where the system gradually approaches global failure through several intermediate failure events. We find that if a histogram of the number of elements failing simultaneously is recorded, it follows a power law with an exponent that crosses over from one value to a very different value when the system is close to global failure. This crossover is, then, the signature of imminent breakdown. The first system studied here is a bundle of many fibers [9,10] with stochastically distributed fiber strengths. This model is sufficiently simple that an analytic treatment is feasible [11–18]. The second system is a fuse model [1], a two-dimensional lattice in which the bonds are fuses, i.e., Ohmic resistors with stochastically distributed threshold values. This model must be analyzed numerically. Both models exhibit similar crossovers as signal of imminent breakdown.

The paper is organized as follows. In Sec. II we present numerical evidence for the crossover in the fiber bundle model, backed up by analytic derivations. We pay particular attention to the burst properties just before complete breakdown. Cascading failures in a fuse model is the theme of Sec. III.

II. THE FIBER BUNDLE MODEL

A. Numerical evidence

A bundle of many fibers with stochastically distributed fiber strengths, and clamped at both ends, is a much-studied model [9–18] for failure avalanches. In its classical version, a ruptured fiber carries no load and the increased stresses caused by a failed element are shared equally by all the surviving fibers. The maximal loads x_n that the fibers $n=1,2,\ldots,N$ are able to carry are picked independently with a probability density $p(x)$:

$$\mathrm{Prob}(x \leq x_n < x + dx) = p(x)dx. \tag{1}$$

A main result for this model is that under mild restrictions on the fiber strength distribution the expected number $D(\Delta)$ of burst avalanches in which Δ fibers fail simultaneously is governed by a universal power law [11]

$$D(\Delta) \propto \Delta^{-\xi} \tag{2}$$

for large Δ, with $\xi=5/2$. However, we will show that when the whole bundle is close to breaking down the exponent

*Electronic address: pradhan.srutarshi@ntnu.no
†Electronic address: alex.hansen@ntnu.no
‡Electronic address: per.hemmer@ntnu.no

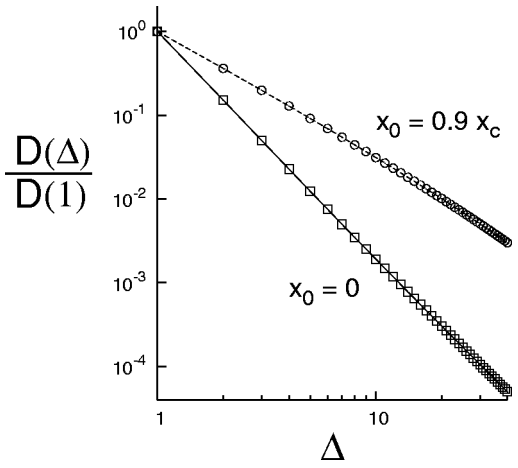

FIG. 1. The distribution of bursts for the strength distribution (5) with $x_0=0$ and $x_0=0.9x_c$. The figure is based on 50 000 samples with $N=10^6$ fibers.

crosses over to a lower value. Such a complete breakdown can be estimated as follows. The force $F(x)$ that the bundle is able to withstand when all fibers with strengths less than x have ruptured is proportional to the number of surviving fibers times the strength,

$$F(x) = NxQ(x), \tag{3}$$

where

$$Q(x) = \int_x^\infty p(x)dx \tag{4}$$

is the expected fraction of fibers with strengths exceeding x. As an example, assume the threshold distribution $p(x)$ to be uniform in an interval (x_0,x_m),

$$p(x) = \begin{cases} (x_m - x_0)^{-1} & \text{for } x_0 \le x \le x_m, \\ 0 & \text{otherwise.} \end{cases} \tag{5}$$

In this case we obtain

$$F(x) = N\frac{x(x_m - x)}{x_m - x_0}, \tag{6}$$

which has a maximum at $x_c=x_m/2$. In general we call $F(x)$ the *average* force and the value corresponding to the maximum of $F(x)$ the *critical* threshold value x_c. If $F(x)$ given by (3) were the actual force, the bundle would break down when x reaches the value x_c. By the existence of fluctuations, however, the maximum value of the force may actually occur at a slightly different (probably higher) value of x.

We want to study burst avalanches when the weakest fiber x_0 is close to the critical value x_c. In Fig. 1 we show results for $D(\Delta)$ for the uniform distribution with $x_0=0.9x_c$. For comparison, simulation results with $x_0=0$ are shown. In both cases $D(\Delta)$ shows a power-law decay, apparently with an exponent $\xi=3/2$ for $x_0=0.9x_c$ in contrast to the standard exponent $\xi=5/2$ for the $x_0=0$ case.

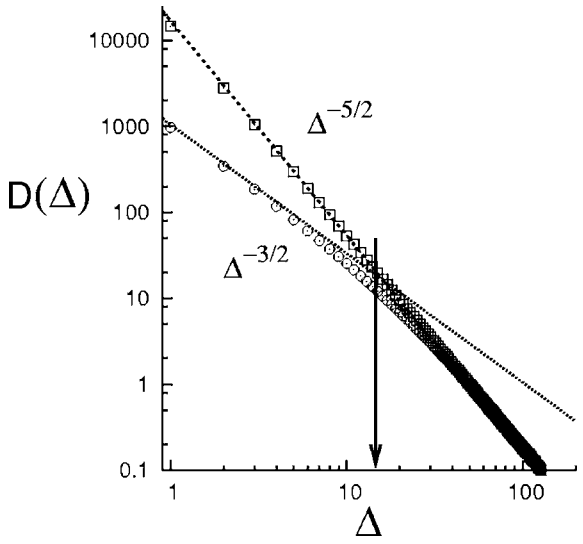

FIG. 2. The distribution of bursts for the Weibull distribution $Q(x)=\exp[-(x-1)^{10}]$, where $1\le x\le\infty$. Again results for the two cases $x_0=1$ (squares) and 1.7 (circles) are displayed ($x_c=1.72\,858$ for this distribution). The figure is based on 50 000 samples with $N=10^6$ fibers and the arrow locates the crossover point $\Delta_c\simeq 14.6$.

In Fig. 2 we show that the same two exponents appear for a much more concentrated threshold distribution, the Weibull distribution. We will in the following explain the results as a crossover phenomenon.

B. Analytical treatment of the crossover

For a bundle of many fibers the number of bursts of length Δ is given by [11]

$$\frac{D(\Delta)}{N} = \frac{\Delta^{\Delta-1}e^{-\Delta}}{\Delta!}\int_0^{x_c} p(x)r(x)[1-r(x)]^{\Delta-1}\exp[\Delta r(x)]dx, \tag{7}$$

where

$$r(x) = 1 - \frac{xp(x)}{Q(x)} = \frac{1}{Q(x)}\frac{d}{dx}[xQ(x)]. \tag{8}$$

From the last expression we see that $r(x)$ vanishes at the point x_c where the average force expression (3) is maximal. If we have a situation in which the weakest fiber has its threshold x_0 just a little below the critical value x_c the contribution to the integral in the expression (7) for the burst distribution will come from a small neighborhood of x_c. Since $r(x)$ vanishes at x_c it is small here, and we may in this narrow interval approximate the Δ-dependent factors in (7) as follows:

$$(1-r)^\Delta e^{\Delta r} = \exp[\Delta(\ln(1-r)+r)] = \exp\{-\Delta[r^2/2 + O(r^3)]\}$$
$$\approx \exp(-\Delta r(x)^2/2). \tag{9}$$

We also have

$$r(x) \approx r'(x_c)(x - x_c). \tag{10}$$

Inserting everything into Eq. (7), we obtain to dominating order

$$\frac{D(\Delta)}{N} = \frac{\Delta^{\Delta-1}e^{-\Delta}}{\Delta!}\int_{x_0}^{x_c} p(x_c)r'(x_c)(x-x_c)e^{-\Delta r'(x_c)^2(x-x_c)^2/2}dx$$
$$= \frac{\Delta^{\Delta-2}e^{-\Delta}p(x_c)}{|r'(x_c)|\Delta!}\left[e^{-\Delta r'(x_c)^2(x-x_c)^2/2}\right]_{x_0}^{x_c}$$
$$= \frac{\Delta^{\Delta-2}e^{-\Delta}}{\Delta!}\frac{p(x_c)}{|r'(x_c)|}(1-e^{-\Delta/\Delta_c}), \quad (11)$$

with

$$\Delta_c = \frac{2}{r'(x_c)^2(x_c-x_0)^2}. \quad (12)$$

By use of the Stirling approximation $\Delta! \simeq \Delta^\Delta e^{-\Delta}\sqrt{2\pi\Delta}$—a reasonable approximation even for small Δ—the burst distribution (11) may be written as

$$\frac{D(\Delta)}{N} = C\Delta^{-5/2}(1-e^{-\Delta/\Delta_c}), \quad (13)$$

with a nonzero constant

$$C = (2\pi)^{-1/2}p(x_c)/|r'(x_c)|. \quad (14)$$

We see from (13) that there is a crossover at a burst length around Δ_c, so that

$$\frac{D(\Delta)}{N} \propto \begin{cases} \Delta^{-3/2} & \text{for } \Delta \ll \Delta_c, \\ \Delta^{-5/2} & \text{for } \Delta \gg \Delta_c. \end{cases} \quad (15)$$

We have thus shown the existence of a crossover from the generic asymptotic behavior $D \propto \Delta^{-5/2}$ to the power law $D \propto \Delta^{-3/2}$ near criticality, i.e., near global breakdown. The fact that there may be a different burst distribution exponent near breakdown has been noted by Sornette (see Ref. [1] and references therein), and observed by Zapperi *et al.* [19] for a fuse model. The crossover is a universal phenomenon, independent of the threshold distribution $p(x)$. In addition we have located where the crossover takes place.

For the uniform distribution $\Delta_c = (1-x_0/x_c)^{-2}/2$, so for $x_0 = 0.9x_c$, we have $\Delta_c = 50$. The final asymptotic behavior is therefore not visible in Fig. 1. The crossover is seen better for $x_0 = 0.8x_c$, as in Fig. 3. Now a crossover is clearly observed near $\Delta = \Delta_c = 12.5$, as expected.

The simulation results shown in the figures are based on *averaging* over a large number of fiber bundles with moderate N. For applications it is important that crossover signals are seen also in a single sample. We show in Fig. 4 that equally clear power laws are seen for a *single* fiber bundle when N is large.

C. Sampling a finite interval

Above we have explained the crossover in burst distributions in which all bursts up to complete breakdown are counted. For the purpose of finding signals of imminent global failure one must, of course, determine burst distributions short of complete breakdown. Consequently we are interested in sampling a finite interval (x_0, x_f), with $x_f < x_c$. When the interval is in the neighborhood of x_c we have, as in Eq. (11),

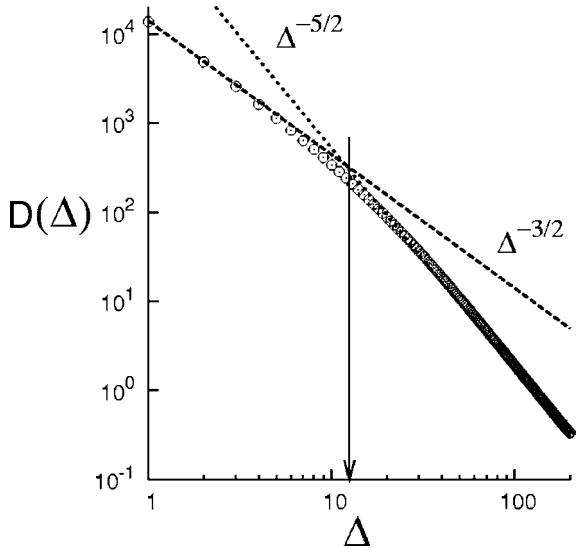

FIG. 3. The distribution of bursts for the uniform threshold distribution (5) with $x_0 = 0.80x_c$. The figure is based on 50 000 samples with $N = 10^6$ fibers. The straight lines represent two different power laws, and the arrow locates the crossover point $\Delta_c \simeq 12.5$.

$$\frac{D(\Delta)}{N} \simeq \frac{\Delta^{\Delta-2}e^{-\Delta}p(x_c)}{|r'(x_c)|\Delta!}\left[e^{-r'(x_c)^2(x-x_c)^2\Delta/2}\right]_{x_0}^{x_f} \quad (16)$$

$$\simeq C\Delta^{-5/2}(e^{-\Delta(x_c-x_f)^2/a} - e^{-\Delta(x_c-x_0)^2/a}), \quad (17)$$

with $a = 2/r'(x_c)^2$.

This shows a crossover:

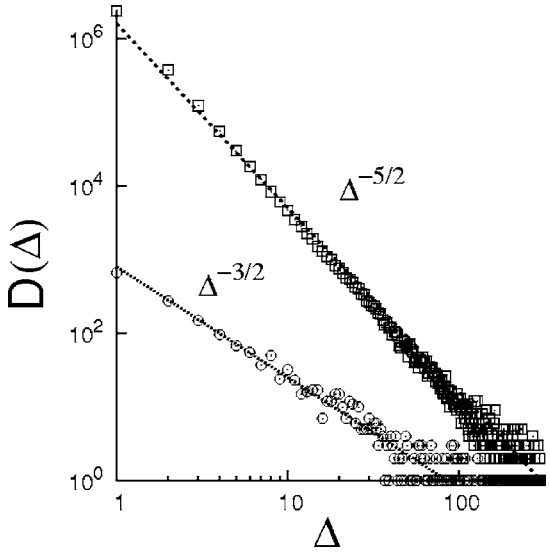

FIG. 4. Avalanche distribution for the uniform threshold distribution (5) for a single fiber bundle with 10^7 fiber: all avalanches (squares) and avalanches near the critical point (circles). Dotted straight lines are the best fits to the power laws.

$$\frac{D(\Delta)}{N} = \begin{cases} \tilde{C}\Delta^{-3/2} & \text{for } \Delta \ll a/(x_c - x_0)^2, \\ C\Delta^{-5/2} & \text{for } a/(x_c - x_0)^2 \ll \Delta \ll a/(x_c - x_f)^2, \end{cases} \tag{18}$$

with a final exponential behavior when $\Delta \gg a/(x_c - x_f)^2$. Here $\tilde{C} = Ca^{-1}[(x_c - x_f)^2 - (x_c - x_0)^2]$.

The 3/2 power law will be seen only when the beginning of the interval, x_0, is close enough to the critical value x_c to create a sizable range of bursts obeying this power law. Observing the 3/2 power law is therefore a signal of imminent system breakdown.

D. Burst avalanches at criticality

Precisely at criticality ($x_0 = x_c$) we have $\Delta_c = \infty$, and consequently the $\xi = 5/2$ power law is no longer present. We will now argue, using a random walk representation, that at criticality the burst distribution follows a 3/2 power law. The load on the bundle when the kth fiber with strength x_k is about to fail is proportional to

$$F_k = x_k(N - k + 1). \tag{19}$$

The expectation value of this is the average force equation (3). At criticality the F is, on the average, stationary. It is, however, the *fluctuations* of this load that now determine the size of the bursts. It has been shown [12] that the probability $\rho(f)df$ that the difference $F_{k+1} - F_k$ lies in the interval $(f, f + df)$ is given by

$$\rho(f) = \begin{cases} \dfrac{1 - r(x_k)}{x_k} e^{-(1-r(x_k))(1+f/x_k)} & \text{for } f \geq -x_k, \\ 0 & \text{for } f < -x_k, \end{cases} \tag{20}$$

where $r(x)$ is given by Eq. (8). At criticality $r = 0$, resulting in

$$\rho_c(f) = \begin{cases} x_c^{-1} e^{-1} e^{-f/x_c} & \text{for } f \geq -x_c, \\ 0 & \text{for } f < -x_c. \end{cases} \tag{21}$$

This can be considered as the step probability in a random walk. The random walk is unsymmetrical, but *unbiased*, $\langle f \rangle = 0$, as it should be at criticality.

A first burst of size Δ corresponds to a random walk in which the position after each of the first $\Delta - 1$ steps is lower than the starting point, but after step no. Δ the position of the walker exceeds the starting point. The probability of this equals

$$\text{Prob}(\Delta) = \int_{-x}^{0} \rho(f_1)df_1 \int_{-x}^{-f_1} \rho(f_2)df_2 \int_{-x}^{-f_1-f_2} \rho(f_3)df_3 \cdots \int_{-x}^{-f_1-f_2-\cdots-f_{\Delta-2}} \rho(f_{\Delta-1})df_{\Delta-1} \int_{-f_1-f_2-\cdots-f_{\Delta-1}}^{\infty} \rho(f_\Delta)df_\Delta. \tag{22}$$

The last integral is easy. By means of (21) we have

$$\int_{-f_1-f_2-\cdots-f_{\Delta-1}}^{\infty} \rho(f_\Delta)df_\Delta = e^{-1}e^{(f_1+f_2+\cdots+f_{\Delta-1})/x}. \tag{23}$$

Since $\rho(f)e^{f/x} = e^{-1}/x$ we end up with

$$\text{Prob}(\Delta) = e^{-\Delta} \int_{-1}^{0} df_1 \int_{-1}^{-f_1} df_2 \times \int_{-1}^{-f_1-f_2} df_3 \cdots \int_{-1}^{-f_1-f_2-\cdots-f_{\Delta-2}} df_{\Delta-1}. \tag{24}$$

For simplicity we have put $x_c = 1$, since the quantity x_c simply determines the scale of the steps, and here it is only relative step lengths that matters.

In the Appendix we have evaluated the expression (22), with the result

$$\text{Prob}(\Delta) = \frac{e^{-\Delta}\Delta^{\Delta-1}}{\Delta!} \simeq \frac{1}{\sqrt{2\pi}}\Delta^{-3/2}, \tag{25}$$

and also shown that these probabilities satisfy

$$\sum_{\Delta=1}^{\infty} \text{Prob}(\Delta) = 1. \tag{26}$$

The result (26) is strictly applicable only in the limit $N \to \infty$; for finite N the sum has to be slightly less than unity. For one thing Δ cannot exceed N, and breaking off the sum at $\Delta = N$ would decrease the sum by an amount of order $N^{-1/2}$. In reality, the sum deviates from unity by an amount of order $N^{-1/3}$ (see the following section).

The simulation results in Fig. 5 are in excellent agreement with the distribution (25). At the completion of a burst the force, i.e., the excursion of the random walk, is larger than all previous values. Therefore one may use this point as a new starting point to find, by the same calculation, the distribution of the next burst, etc. Consequently the complete burst distribution is essentially proportional to $\Delta^{-3/2}$ as expected. In the next section we study the burst distribution at criticality in more detail, in particular its dependence upon the bundle size N.

E. Finite-size effects at criticality

When the fiber bundle is subcritical the average number of bursts of a given length will be proportional to the bundle size N. When the bundle is critical this is no longer so. Each burst will produce a non-negligible weakening of the bundle, so that the bundle will be slightly more supercritical. Then the probability of a total breakdown will increase, and the

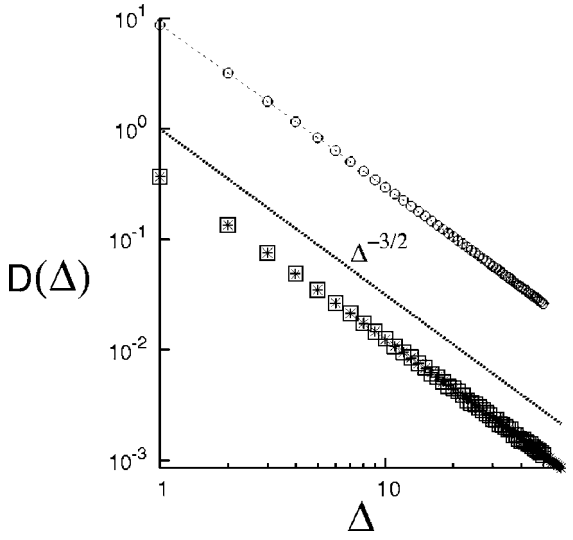

FIG. 5. Distribution of first bursts (squares) and total bursts (circles) for the critical strength distribution (5) with $x_0=x_c$. The simulation results are based on 10^6 samples with $N=80\,000$ fibers. The star symbol stands for the analytic result (25).

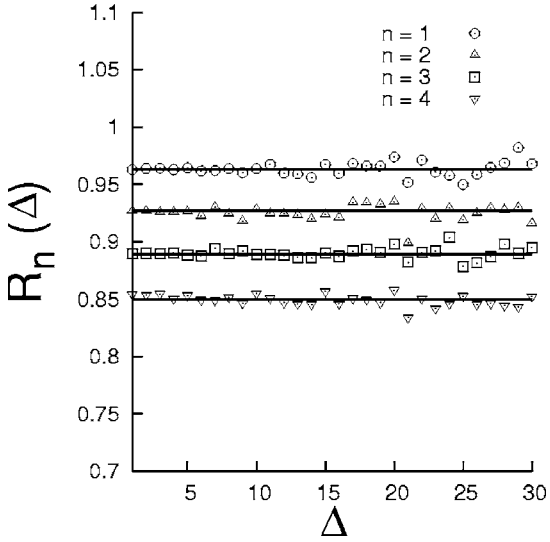

FIG. 6. Simulation results for the Δ dependence of the ratios (28). We have used the uniform strength distribution at criticality. The figure is based on 10^7 samples with $N=40\,000$ fibers. The straight lines are the average values.

probability of a burst of finite length decreases.

To study this quantitatively we therefore have to specify not only the size Δ of a burst, but also if it is the first burst after starting, the second, the third, etc. Let $P_n(\Delta)$ be the number of bursts of size Δ that occur as the nth burst. If we start precisely at criticality, we have already calculated

$$P_1(\Delta) = \frac{e^{-\Delta}\Delta^{\Delta-1}}{\Delta!}, \tag{27}$$

by Eq. (25). We will in particular study how the probability decreases with increasing n, so we form the ratios

$$R_n(\Delta) = \frac{P_n(\Delta)}{P_1(\Delta)}. \tag{28}$$

We start by investigating the Δ dependence of these ratios, and for simplicity we work with the critical uniform threshold distribution throughout this subsection. In Fig. 6 we have plotted $R_n(\Delta)$ versus Δ. The ratios (28) depend upon n, but surprisingly we cannot detect any systematic dependence on Δ. We may therefore obtain the dependence upon n and N by sticking to one fixed Δ; for simplicity we take $\Delta=1$.

In Fig. 7 we have plotted $R_n(1)$ for four different values of N and for $n=2$, 3, 4, and 5. The figure shows that $R_n(1)$ for each value of n apparently depends linearly on $N^{-1/3}$ and that $1-R_n(1)$ apparently is proportional to $n-1$. Empirically the data can reasonably well be represented by

$$R_n(1) = 1 - 1.27(n-1)N^{-1/3}. \tag{29}$$

More generally we may assume that the linear function is a limiting form of a more general function:

$$R_n(1) = F(x) \quad \text{with } x = (n-1)N^{-1/3}, \tag{30}$$

where $F(0)=1$ and $F(x)\simeq 1-1.27x$ for small x. For large x we expect $F(x)$ to approach zero.

If (30) is correct we should have a data collapse onto the single curve $F(x)$. Figure 8 shows that the data collapse works well. In order to test the function $F(x)$ beyond its initial linear behavior, we have added a few points with larger values of x. In addition to the results of Fig. 7(a) we have obtained results for $n=10$, 20, and 30, with $N=5000$, 10 000, and 80 000 [Fig. 7(b)].

$F(x)$ is seen to decrease towards zero for increasing x, and the empirical expression

$$F(x) \simeq \frac{2}{1+e^{2.54x}} \tag{31}$$

seems to represent the data in Fig. 8 very well.

The relation (30) implies some interesting consequences. Let us first consider the total number of bursts of a given size:

$$\begin{aligned} D(\Delta) &= \sum_n P_n(\Delta) = P_1(\Delta)\sum_n R_n(\Delta) \simeq P_1(\Delta)\sum_n R_n(1) \\ &= P_1(\Delta)\sum_n F[(n-1)N^{-1/3}] \\ &\simeq P_1(\Delta)\int_1^\infty F[(n-1)N^{-1/3}]dn \\ &= P_1(\Delta)N^{1/3}\int_0^\infty F(x)dx. \end{aligned} \tag{32}$$

We have used that $R_n(\Delta)$ is essentially independent of Δ (Fig. 6), and that due to smallness of $N^{-1/3}$ we may replace summation by integration.

The conclusion is that the total number of bursts should scale as $N^{1/3}$. The simulation results presented in Table I are in excellent agreement with this N dependence.

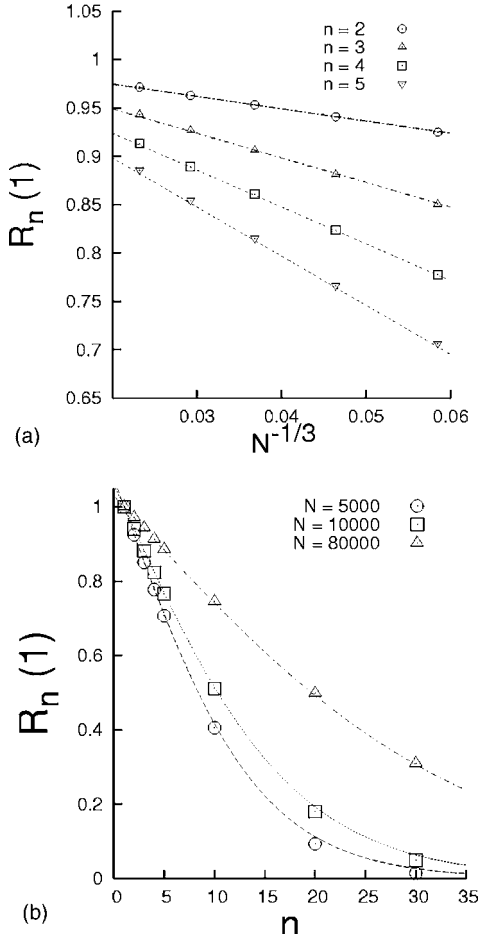

FIG. 7. Simulation results for the ratios $R_n(1)$ as function of $N^{-1/3}$ (a) and as function of n (b). The dotted lines represent the functional forms (29) (a) and (31) (b). The results are based on 10^7 samples, except for $N=80\,000$ (10^6 samples).

According to (32) the numbers in Table I should all be the same (or nearly the same) and represent the integral of F. The integral of the empirical representation (31) of $F(x)$ equals 0.546, in close agreement with the results in the table.

We have also recorded the number D(failure) of *immediate* failures of the fiber bundle (i.e., with no finite bursts at all). We have presented the numbers in Table I. The number of immediate failures decreases with increasing N as $N^{-1/3}$. The reason for the decrease is that in a large bundle it is more probable to find a fiber sufficiently strong to prevent immediate failure.

It remains a challenge to derive these finite-size scaling results analytically.

III. BURST AVALANCHES IN THE FUSE MODEL

Let us test the crossover phenomenon in a more complex situation than for fiber bundles. We have studied burst distributions in the fuse model [1]. It consists of a lattice in which each bond is a fuse, i.e., an Ohmic resistor as long as the electric current it carries is below a threshold value. If the threshold is passed, the fuse burns out irreversibly. The

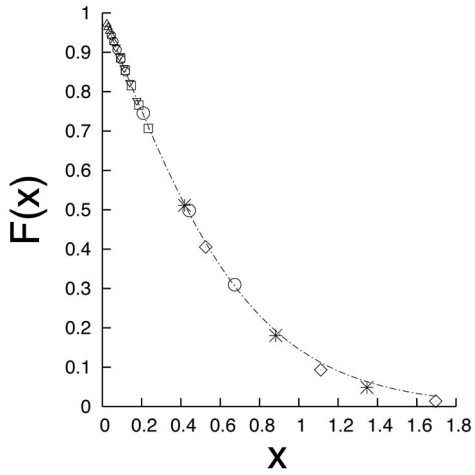

FIG. 8. The data collapse onto a single curve $F(x)$ [dotted line represents Eq. (31)] where $x=(n-1)\times N^{-1/3}$. We have taken $N=5000$, 10 000, 20 000, 40 000, 80 000 and $n=2$, 3, 4, 5, 10,20,30. Averages are taken over 10^7 samples, except for $N=80\,000$ (10^6 samples).

threshold t of each bond is drawn from an uncorrelated distribution $p(t)$. The lattice is placed between electrical bus bars and an increasing current is passed through it. Numerically, the Kirchhoff equations are solved with a voltage difference between the bus bars set to unity. The ratio between current i_j and threshold t_j for each bond j is calculated and the bond having the largest value, $\max_j(i_j/t_j)$, is identified and subsequently irreversibly removed. The lattice is a two-dimensional square one placed at 45° with regard to the bus bars. The threshold distribution is uniform on the unit interval. All fuses have the same resistance. The burst distribution follows the power law (2) with $\xi=3$, which is consistent with the value reported in recent studies [19,20]. We show the histogram in Fig. 9. With a system size of 100×100, 2097 fuses blow on the average before catastrophic failure sets in. When measuring the burst distribution only after the first 2090 fuses have blown, a different power law is found, this time with $\xi=2$. After 1000 blown fuses, on the other hand, ξ remains the same as for the histogram recording the entire failure process (see Fig. 9). Zapperi *et al.* [19], who study the fuse model on the diamond and the triangular lattices, find significant variation with the lattice type. Their exponent values for the diamond lattice are 2.75 and 1.90, not very different from the values 3.0 and 2.0 in our Fig. 9.

In Fig. 10, we show the power dissipation E in the network as a function of the number of blown fuses. The dissi-

TABLE I. Simulation results.

N	5000	10000	20000	40000	80000
$N^{-1/3}D(1)/P(1)$	0.545	0.546	0.546	0.550	0.550
$N^{-1/3}D(2)/P(2)$	0.546	0.549	0.550	0.547	0.552
$N^{-1/3}D(3)/P(3)$	0.542	0.550	0.548	0.547	0.546
$N^{-1/3}D(4)/P(4)$	0.538	0.548	0.544	0.548	0.546
$N^{-1/3}D(5)/P(5)$	0.542	0.545	0.546	0.548	0.550
$N^{1/3}D$(failure)	1.2154	1.2319	1.2346	1.2293	1.2307

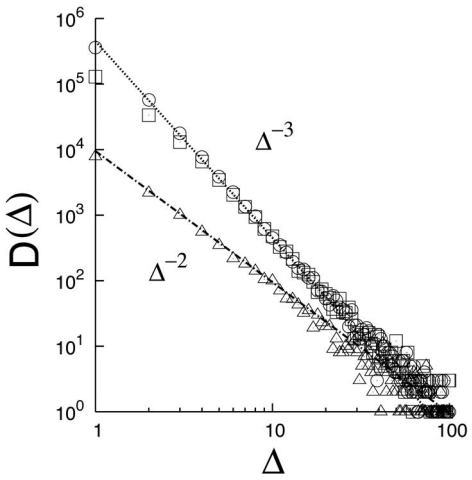

FIG. 9. Burst distribution in the fuse model: System size is 100×100 and averages are taken for 300 samples. On the average, catastrophic failure sets in after 2097 fuses have blown. The circles denote the burst distribution measured throughout the entire breakdown process. The squares denote the burst distribution based on bursts appearing after the first 1000 fuses have blown. The triangles denote the burst distribution after 2090 fuses have blown. The two straight lines indicate power laws with exponents $\xi=3$ and 2, respectively.

pation is given as the product of the voltage drop across the network V times the total current that flows through it. In Fig. 11, we show the power dissipation as a function of the total current. The breakdown process starts by following the lower curve, and follows the upper curve returning to the origin. It is interesting to note the linearity of the unstable branch of this curve. In Fig. 12, we record the avalanche distribution for power dissipation, $D_d(\Delta)$. Recording, as before, the avalanche distribution throughout the entire process and recording only close to the point at which the system catastrophically fails, results in two power laws, with exponents $\xi=2.7$ and 1.9, respectively. It is interesting to note that in this case there is not a difference of unity between the two exponents. The power dissipation in the fuse model corresponds to the stored elastic energy in a network of elastic

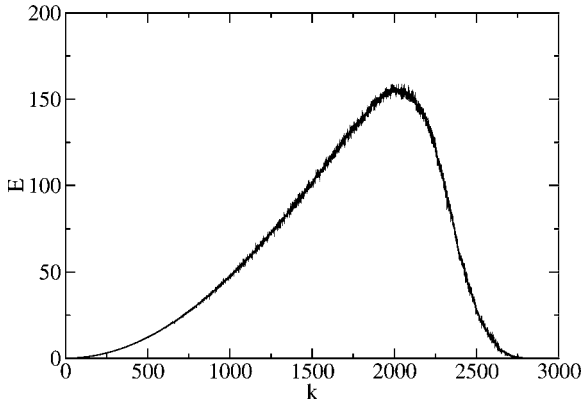

FIG. 10. Power dissipation E as a function of the number of broken bonds in the fuse model. The system size and number of samples are the same as in Fig. 9.

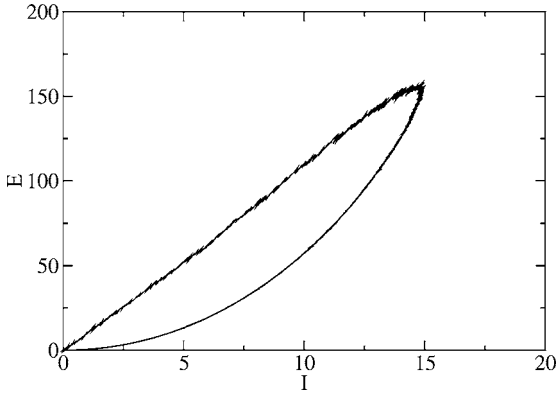

FIG. 11. Power dissipation E as a function of the total current I flowing in the fuse model. The system size and number of samples are the same as in Fig. 9.

elements. Hence, the power dissipation avalanche histogram would in the mechanical system correspond to the released energy. Such a mechanical system would serve as a simple model for earthquakes.

The Gutenberg-Richter law [2–4] relating the frequency of earthquakes with their magnitude is essentially a measure of the elastic energy released in the earth's crust, as the magnitude of an earthquake is the logarithm of the elastic energy released. Hence, the power dissipation avalanche histogram $D_d(\Delta)$ in the fuse model corresponds to the quantity that the Gutenberg-Richter law addresses in seismology. Furthermore, the power-law character of $D_d(\Delta)$ is consistent with the form of the Gutenberg-Richter law. It is then intriguing that there is a change in exponent ξ also for this quantity when failure is imminent. Recently Kawamura [22] has observed a similar decrease in exponent value of the local magnitude distribution of earthquakes in Japan as the mainshock is approached. This encourages the possibility of using the crossover signals as a practical warning sign.

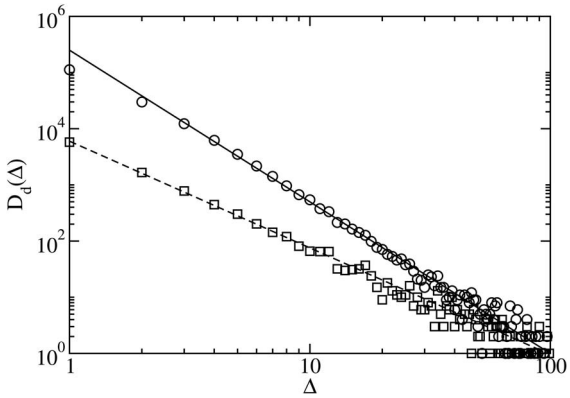

FIG. 12. The power dissipation avalanche histogram $D_d(\Delta)$ in the fuse model. The slopes of the two straight lines are −2.7 and −1.9, respectively. The circles show the histogram of avalanches recorded through the entire process, whereas the squares show the histogram recorded only after 2090 fuses have blown. The system size and number of samples are the same as in Fig. 9.

IV. CONCLUDING REMARKS

We have studied the avalanche distribution $D(\Delta) \propto \Delta^{-\xi}$ in the fiber bundle model, and have shown analytically that close to complete breakdown it exhibits a crossover behavior between two power laws with exponents $\xi=5/2$ and $3/2$. This crossover behavior is universal in the sense that, under mild assumptions, it does not depend on the statistical distribution of the thresholds. In the critical situation an argument based on a unbiased unsymmetrical random-walk scenario explains the exponent $\xi=3/2$. Near criticality the avalanche distribution depends on the system size in a nontrivial way. For this case we present quantitative results that may be summarized by a finite-size scaling function [Eq. (31)].

The crossover behavior is not limited to the fiber bundle model. We show numerically that the same crossover phenomenon occurs in the two-dimensional fuse model. The exponents are different, though, $\xi=2$ near breakdown and $\xi=3$ away from it. For this fuse model the power dissipation avalanches show a crossover, with power law exponents $\xi=2.7$ and $\xi=1.9$. Such crossovers signal that catastrophic failure is imminent, and has therefore a strong potential as a useful detection tool for systems with slow buildup of tension. Some of the present results have already been published as a Letter [18].

ACKNOWLEDGMENTS

S.P. thanks the Research Council of Norway (NFR) for financial support through Grant No. 166720/V30.

APPENDIX: PROOF OF EQ. (25)

We evaluate here the multiple integral in Eq. (22)

$$\mathrm{Prob}(\Delta) = e^{-\Delta} \int_{-1}^{0} df_1 \int_{-1}^{-f_1} df_2 \int_{-1}^{-f_1-f_2} \times df_3 \cdots \int_{-1}^{-f_1-f_2-\cdots-f_{\Delta-2}} df_{\Delta-1}. \tag{A1}$$

We introduce the new variables

$$\begin{aligned} y_1 &= -f_1, \\ y_2 &= -f_1 - f_2, \\ \cdots &= \cdots, \\ y_{\Delta-1} &= -f_1 - f_2 - \cdots - f_{\Delta-1}, \end{aligned} \tag{A2}$$

satisfying

$$\begin{aligned} 0 &\le y_1 \le 1, \\ 0 &\le y_2 \le 1 + y_1, \\ 0 &\le y_i \le 1 + y_{i+1}, \quad i = 2,3,\ldots,\Delta-1. \end{aligned} \tag{A3}$$

Then

$$\mathrm{Prob}(\Delta) = e^{-\Delta} \int_0^1 dy_1 \int_0^{1+y_1} dy_2 \int_0^{1+y_2} \cdots \int_0^{1+y_{\Delta-2}} dy_{\Delta-1}. \tag{A4}$$

Defining $V_0(y)=1$, and

$$V_d(y) = \int_0^{1+y} V_{d-1}(z)\,dz, \tag{A5}$$

we have

$$\mathrm{Prob}(\Delta) = e^{-\Delta} V_{\Delta-1}(0). \tag{A6}$$

Equation (A5) can be solved by iteration. By calculating the first polynomials $V_n(y)$ one is led to assume

$$V_{d-1}(y) = \frac{1}{d!} \sum_{i=1}^{d-1} d^{d-i-1} \binom{d-1}{i} (i+1) y^i. \tag{A7}$$

Suppose this is valid up to some value of $d-1$. Then use (A5) to compute V_d. The integration is trivial, leaving

$$\begin{aligned} V_d(y) &= \frac{1}{d!} \sum_{i=0}^{d-1} \binom{d-1}{i} d^{d-i-1} (1+y)^{i+1} \\ &= \frac{1}{d!} \sum_{i=0}^{d-1} \sum_{m=0}^{i+1} \binom{d-1}{i} \binom{i+1}{m} d^{d-i-1} y^m \\ &= \frac{1}{d!} \sum_{m=0}^{d} \sum_{i=m-1}^{d-1} \binom{d-1}{i} \binom{i+1}{m} d^{d-i-1} y^m \\ &= \frac{1}{d!} \sum_{m=0}^{d} S(m) y^m, \end{aligned} \tag{A8}$$

with

$$S(m) = \sum_{i=m-1}^{d-1} \binom{d-1}{i} \binom{i+1}{m} d^{d-i-1}. \tag{A9}$$

Since

$$\binom{i+1}{m} = \binom{i}{m-1} + \binom{i}{m} \tag{A10}$$

and

$$\binom{a}{b} = 0 \quad \text{for } b < 0 \text{ or } b > a, \tag{A11}$$

we may write

$$S(m) = \sum_{i=0}^{d-1} \binom{d-1}{i} \left[\binom{i}{m} + \binom{i}{m-1} \right] d^{d-i-1}. \tag{A12}$$

To evaluate $S(m)$ we differentiate the binomial expression

$$\sum_{i=0}^{d-1} \binom{d-1}{i} x^1 = (1+x)^{d-1} \tag{A13}$$

m times with respect to x:

$$\sum_{i=0}^{d-1} \binom{d-1}{i} i(i-1)\cdots(i-m+1)x^{i-m} = (d-1)(d-2)\cdots(d-m)(1+x)^{d-1-m}, \quad \text{(A14)}$$

or

$$\sum_{i=0}^{d-1} \binom{d-1}{i}\binom{i}{m} m\,!\, x^{i-m} = \frac{(d-1)!}{(d-m-1)!}(1+x)^{d-1-m}. \quad \text{(A15)}$$

Putting now $x=1/d$, and multiplying both sides of the equation by $d^{d-1-m}/m!$, we obtain

$$s(m) \equiv \sum_{i=0}^{d-1} \binom{d-1}{i}\binom{i}{m} d^{d-i-1} = \frac{(d-1)!}{(d-m-1)\,!\,m!}(1+d)^{d-1-m}. \quad \text{(A16)}$$

By Eq. (A12) then

$$S(m) = s(m) + s(m-1) = \binom{d}{m}(1+d)^{d-m}(1+m)/(1+d). \quad \text{(A17)}$$

Finally Eq. (A8) gives

$$V_d(y) = \frac{1}{(1+d)!}\sum_{m=0}^{d} \binom{d}{m}(d+1)^{d-m}(1+m)y^m. \quad \text{(A18)}$$

Since this is in accordance with the assumption (A7), and since (A7) is correct for $d=2$, the induction proof works.

Finally, using (A6), the probability we seek is

$$\text{Prob}(\Delta) = e^{-\Delta}V_{\Delta-1}(0) = \frac{e^{-\Delta}\Delta^{\Delta-1}}{\Delta!}, \quad \text{(A19)}$$

which is Eq. (25) in the main text.

Let us also sum these probabilities over all burst lengths,

$$S = \sum_{\Delta=1}^{\infty} \frac{e^{-\Delta}\Delta^{\Delta-1}}{\Delta!} = \sum_{\Delta=1}^{\infty} \frac{e^{-\Delta}}{\Delta!}\left[\frac{d^{\Delta-1}}{dS^{\Delta-1}}e^{S\Delta}\right]_{S=0}. \quad \text{(A20)}$$

We may now appeal directly to the theorem of Lagrange [21] to conclude that the sum satisfies the equation

$$S = e^{-1}e^{S}. \quad \text{(A21)}$$

Since Se^{-S} is always less than or equal to e^{-1} for nonnegative S, we must have

$$S = 1, \quad \text{(A22)}$$

which is Eq. (26) in the main text.

[1] *Statistical Models for the Fracture of Disordered Media*, edited by H. J. Herrmann and S. Roux (North-Holland, Amsterdam, 1990).
[2] B. K. Chakrabarti and L. G. Benguigui, *Statistical Physics of Fracture and Breakdown in Disorder Systems* (Oxford University Press, Oxford, 1997).
[3] D. Sornette, *Critical Phenomena in Natural Sciences* (Springer-Verlag, Berlin, 2000).
[4] M. Sahimi, *Heterogeneous Materials II: Nonlinear and Breakdown Properties* (Springer-Verlag, Berlin, 2003).
[5] A. Petri, G. Paparo, A. Vespignani, A. Alippi, and M. Costantini, Phys. Rev. Lett. **73**, 3423 (1994).
[6] A. Garcimartin, A. Guarino, L. Bellon, and S. Ciliberto, Phys. Rev. Lett. **79**, 3202 (1997).
[7] A. Guarino, A. Garcimartin, and S. Ciliberto, Eur. Phys. J. B **6**, 13 (1998).
[8] M. Sahimi and S. Arbabi, Phys. Rev. Lett. **68**, 608 (1992); **77**, 3689 (1996).
[9] F. T. Peirce, J. Text. Inst. **17**, T355 (1926).
[10] H. E. Daniels, Proc. R. Soc. London, Ser. A **183**, 405 (1945).
[11] P. C. Hemmer and A. Hansen, J. Appl. Mech. **59**, 909 (1992).
[12] A. Hansen and P. C. Hemmer, Trends Stat. Phys. **1**, 213 (1994).
[13] M. Kloster, A. Hansen, and P. C. Hemmer, Phys. Rev. E **56**, 2615 (1997).
[14] J. V. Andersen, D. Sornette, and K. T. Leung, Phys. Rev. Lett. **78**, 2140 (1997).
[15] S. Pradhan, P. Bhattacharyya, and B. K. Chakrabarti, Phys. Rev. E **66**, 016116 (2002).
[16] P. Bhattacharyya, S. Pradhan, and B. K. Chakrabarti, Phys. Rev. E **67**, 046122 (2003).
[17] S. Pradhan and A. Hansen, Phys. Rev. E **72**, 026111 (2005).
[18] S. Pradhan, A. Hansen, and P. C. Hemmer, Phys. Rev. Lett. **95**, 125501 (2005).
[19] A. Hansen and P. C. Hemmer, Phys. Lett. A **184**, 394 (1994).
[20] S. Zapperi, P. Nukala, and S. Simunovic, Phys. Rev. E **71**, 026106 (2005).
[21] E. T. Whittaker and G. N. Watson, *A Course of Modern Analysis* (Cambridge University Press, Cambridge, U.K., 1958).
[22] H. Kawamura, e-print cond-mat/0603335.